IEEE Photonics Journal
An IEEE Photonics Society Publication

Open Access

Design and Analysis of a Novel Graphene-Assisted Silica/Polymer Hybrid Waveguide With Thermal–Optical Phase Modulation Structure

Volume 11, Number 2, April 2019

Cheng Qiu
Yu-Bing Wang
Yong-Yi Chen
Yu-Xin Lei
Li Qin
Li-Jun Wang

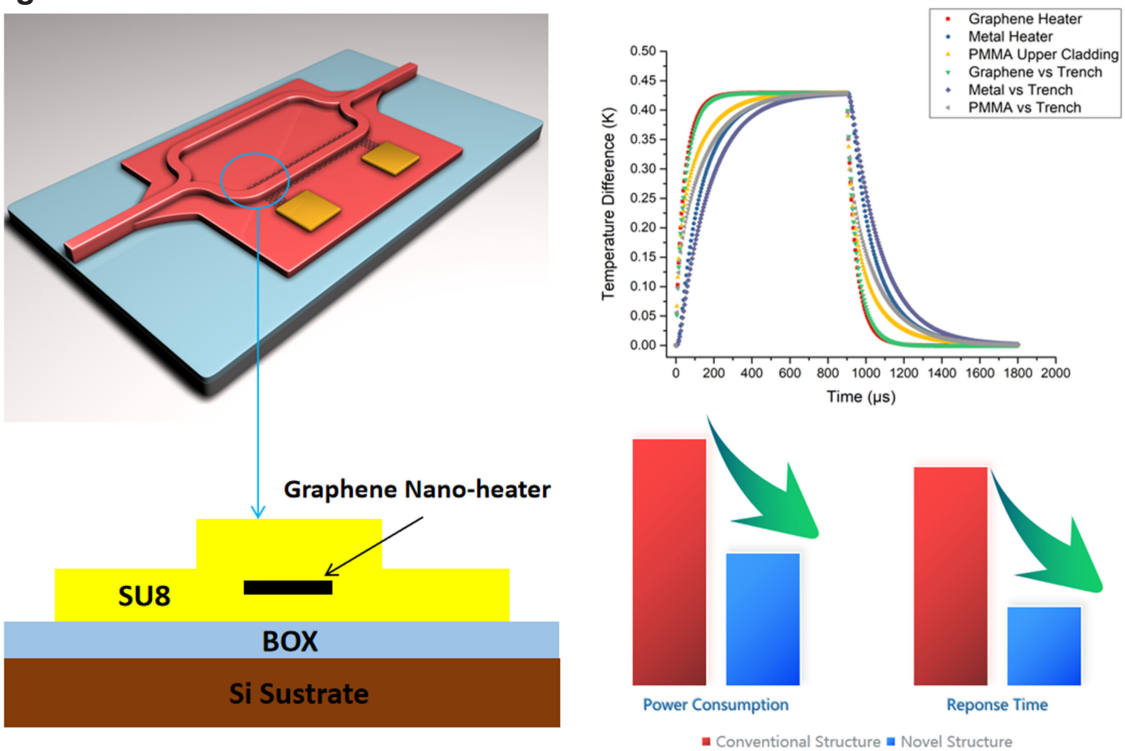

DOI: 10.1109/JPHOT.2019.2909003
1943-0655

Design and Analysis of a Novel Graphene-Assisted Silica/Polymer Hybrid Waveguide With Thermal–Optical Phase Modulation Structure

Cheng Qiu,[1,2] **Yu-Bing Wang**,[1,3] **Yong-Yi Chen**,[1] **Yu-Xin Lei**,[1,2] **Li Qin**,[1] **and Li-Jun Wang**[1]

[1]State Key Laboratory of Luminescence and Application, Changchun Institute of Optics, Fine Mechanics and Physics, Chinese Academy of Sciences, Changchun 130033, China
[2]University of Chinese Academy of Sciences, Beijing 100049, China
[3]State Key Laboratory of Integrated Optoelectronics, Institute of Semiconductors, Chinese Academy of Sciences, Beijing 100083, China

DOI:10.1109/JPHOT.2019.2909003

Manuscript received February 24, 2019; revised March 25, 2019; accepted March 29, 2019. Date of publication April 4, 2019; date of current version April 23, 2019. This work was supported in part by the National Natural Science Foundation of China under Grants 61805236, 51672264, 11874353, 61727822, 61674148, 11604328, 51672264, 61474117, and 61874119 and in part by the Opened Fund of the State Key Laboratory of Integrated Optoelectronics under Grant IOSKL2018KF21. Corresponding author: Yu-Bing Wang (e-mail: wangyubing@ciomp.ac.cn).

Abstract: A novel thermal–optical phase modulation structure based on polymer/silica hybrid waveguide is proposed. Patterned graphene strip is introduced as electric nanoheater in the structure. Finite element method simulation is performed on both thermal and optical field analysis. Results show that response speed is improved by a factor of three and power consumption is reduced by half, in comparison with conventional state-of-art polymer-based phase shifter. This proposed structure is compatible with current complementary metal–oxide–semiconductor power supply standard and has very large design robustness. It shows great application potential on low-power optical switch, modulator and polymer thermal–optical phase arrays.

Index Terms: Graphene nano-heater, thermal optical phase modulator, polymer/silica hybrid planar lightwave circuit.

1. Introduction

Polymer based Planar Lightwave Circuit (PLC) is a very promising platform for applications in high-speed fiber-optical data communications and telecommunications [1]–[5]. Polymer PLC devices based on thermal-optical (TO) effect have been intensively studied during the last decade [6]–[10]. Typical applications include variable optical attenuators [11], optical switches [12], thermal optical resonant filters and optical phase modulators [13], [14].

The general idea of TO devices is tuning refractive index of material of particular area by changing local temperature, so that opt-electric performances of the devices are tuned accordingly. Conventionally, a metallic heater is situated above (or neighboring) the waveguide, where temperature elevation can be achieved through the Joule effect. Fig. 1(a) shows the cross-section of conventional polymer hybrid TO devices. For these types of structures, polymer waveguide is firstly

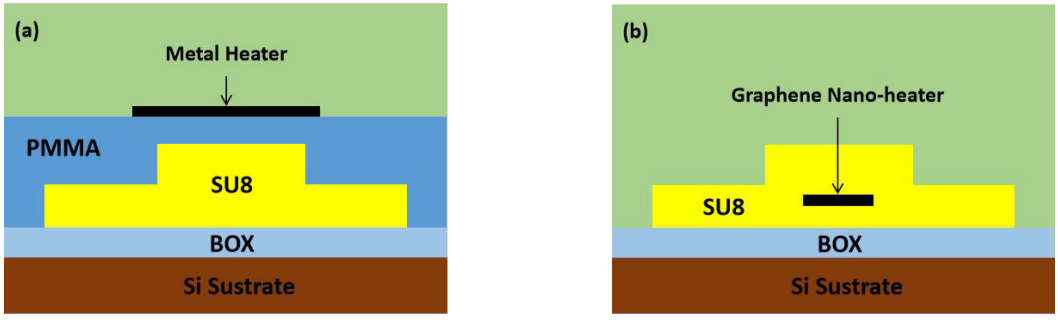

Fig. 1. (a) Conventional polymer hybrid TO devices structure. (b) Proposed novel polymer hybrid TO devices structure in this paper.

fabricated on a Si/SiO2 substrate (in this case, SU8 is employed as the waveguide core material). Another type of polymer (PMMA in this case) is then introduced as upper-cladding layer. Finally, a metallic heater is patterned on the upper-cladding layer. The whole structure operates and produces a phase modulation when the metallic heater is powered on and heat is transferred from the heater to the polymer waveguide core.

A great drawback of such structure is that the upper-cladding layer has to be thick enough (usually around 2 μm) to prevent light absorption from the heater. Considering the small heat conductivity of most polymer materials, this upper-cladding layer would greatly reduce the TO devices' response speed and heating efficiency.

Graphene, the most renowned material, has attracted significant attention since it was born. It has been extensively investigated for many of its extraordinary properties [15]–[25]. Among them, high intrinsic thermal conductivity [26], [27], optical transparency and mechanical flexibility [28]–[30] make graphene a very promising candidate to improve the performances of current TO structure on PLCs.

Several studies have been done to overcome the drawback of the conventional TO structures on many different platforms by introducing graphene material. Yue Sun *et al.* have proposed a TO MZI optical switch structure by using graphene layer as a heat transfer layer on polymer PLC platform [31]. Longhai Yu *et al.* have proposed and fabricated a TO micro-disk resonator by using graphene layer as a heater on Si platform [32]. Sheng Gan *et al.* have proposed and fabricated a TO micro-ring modulator on platform which introduces graphene layer as a nano-heater [33].

In this paper, a new structure and related fabrication process of TO device with assistance of graphene layer on polymer based PLC platform is proposed. This structure is, to the best of our knowledge, the first structure that directly introduce graphene material as nano-heater on PLC platform. A polymer/silica hybrid TO MZI optical switch based on this new structure is designed. Finite Element Method (FEM) analysis is performed on both thermal and optical field distributions. Simulation results compare both the proposed structure and conventional polymer based TO structure, in terms of response speed and power consumption efficiency. According to the results of simulation, TO optical switch with the proposed structure is three times faster in response speed than that of the conventional structure, while consumes only half of power. The proposed structure is then further studied. Design tolerance and device compatibility with current commercial standard of Complementary Metal-Oxide-Semiconductor (CMOS) power supply are discussed.

2. Structure and Fabrication Process Flow

Fig. 1(b) illustrates the structure proposed in this paper. Graphene nano-heaters is deployed inside the polymer waveguide core. On contrary to conventional structure, polymer cladding layer is not necessarily required in this structure.

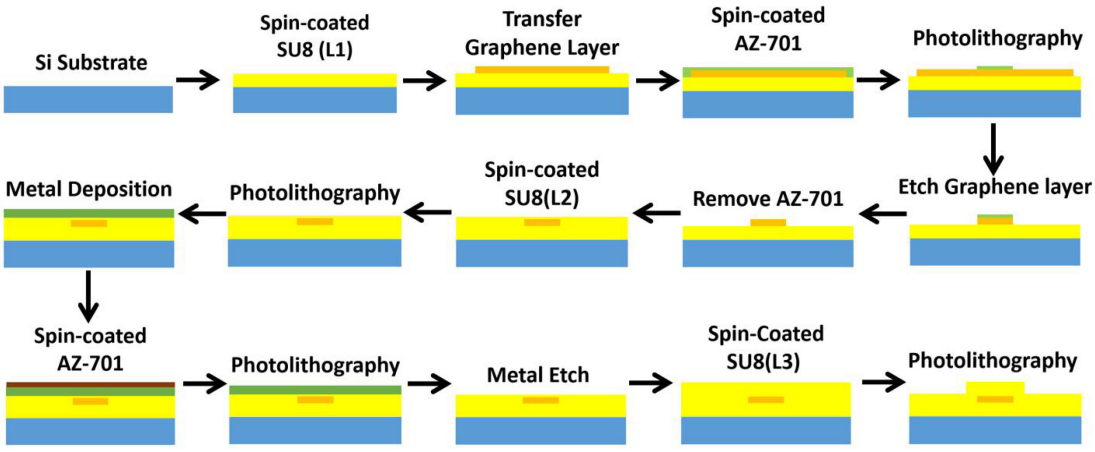

Fig. 2. Fabrication process flow for the novel graphene assisted silica/polymer hybrid waveguide with thermal optical modulated device structure.

A new process flow is also developed to fabricate the proposed structure, as shown in Fig. 2. A slab of polymer(SU8) labeled as L1 is first spin-coated and cured on silicon substrate. Graphene layer is then transferred on L1. Photo-resist(AZ-701) is coated on graphene layer and lithography is performed. Graphene layer is then etched and photo-resist is removed. When the graphene nano-heater layer is patterned, another thin slab of polymer(SU8) labeled as L2 is coated and patterned using lithography. L2 is used as a dielectric separation layer. To form electrode, a layer of metal is then deposit and patterned on L2. Finally, the last polymer layer (SU8) labeled as L3 is coated, patterned by lithography to complete the formation of the ridge waveguide. All the process except graphene transfer step in this flow are standard PLC fabrication process. This will make the approach easy to adapt to the manufacturing standard.

3. Simulation and Results

In order to evaluate the performance of the new structure, a Mach-Zehnder Interference(MZI) optical switch with 10 mm arms shown in Fig. 3 is analyzed.

The reason of implementation of rib waveguide is 1) to achieve minimum optical loss and phase disturbance and 2) to imbed graphene at center of optical mode in order to realize maximum heating efficient.

To make comparison, a group with conventional TO modulate structure is analyzed as while. We also considered the effect of upper-cladding layer, which although is not necessarily required in our proposed structure, and make it another comparison group. Since many studies have shown that air trenches, which are located around waveguide, could effectively reduce the power consumption for TO modulation [34], structures with air trench have been added in each group. In general, six test structures in three comparison groups shown in Fig. 4 have been analyzed and compared in our simulation. The width and the height of the ridge waveguide are set to 3 μm and 1 μm, respectively. The thickness of the upper-cladding layer are set to 2 μm.

Finite Element Method on optical mode analysis is first performed. Fundamental propagation TE mode is obtained. FEM on thermal field is then performed. Heating power in each structure are set at 3 mW. Heat convection coefficient of air and ambient temperature are set to 5 $W{\cdot}m^{-2}{\cdot}K^{-1}$ and 293.15 K, respectively. Simulation results are shown in Fig. 5. The insets at the bottom left corner of each figure are the optical mode of waveguides. Thermal field distributions are shown in the main figures. For readers' convenience, we outlined the optical modes using blue dashed lines, as indications of regions of interest. Green lines represent the position of heaters. The light blue dots, which correspond to the center point of the optical mode, have been chosen as reference points.

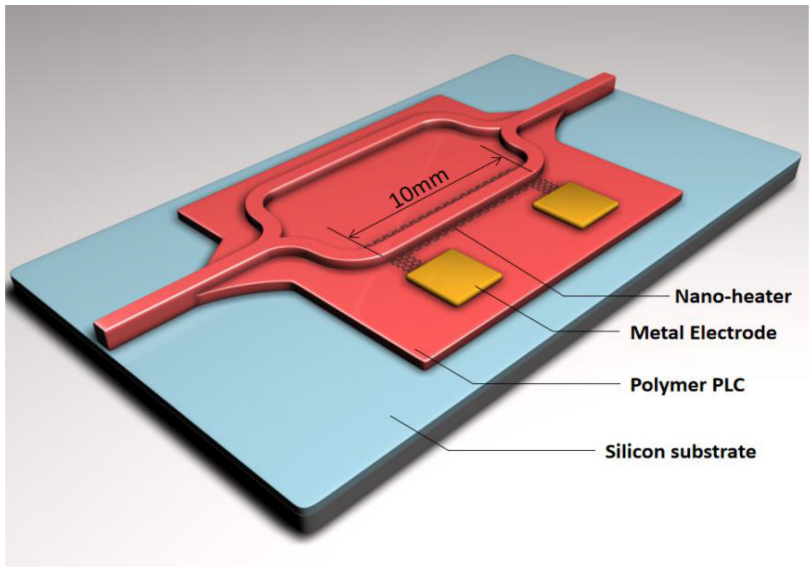

Fig. 3. Hybrid thermal optical Mach-Zehnder Interference switch structure using graphene as nano-heater.

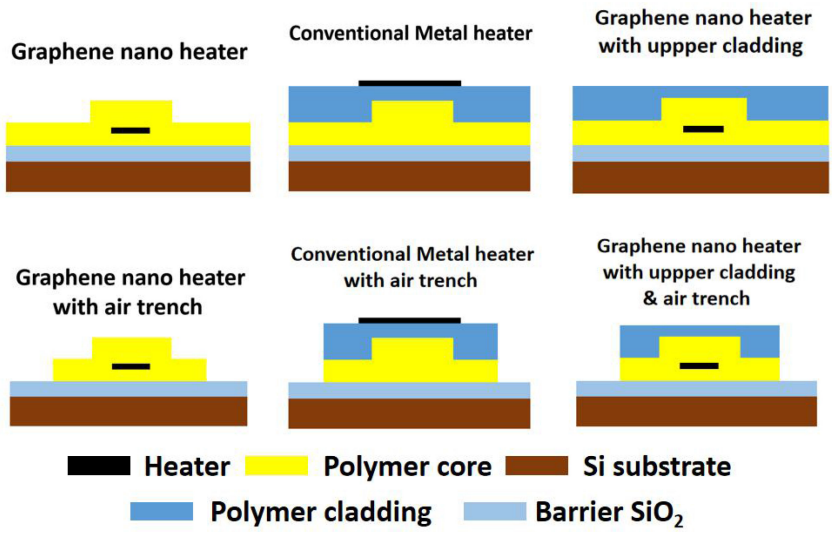

Fig. 4. Schematic cross-section of simulation TO modulation structure.

To analyze the simulation results quantitatively, temperature at reference points on each structure has been compared. Fig. 6 shows the comparison result in terms of temperature difference between reference points and ambient temperature. Since the reference point lies on the center of optical propagation mode, it effectively represents the temperature on the waveguide area.

As shown in Fig. 6, the proposed structure with no upper-cladding has the highest heating efficiency. The temperature difference at the reference point is 0.6 K. The structures with both graphene nano-heater and upper cladding layer have lower heating efficiency, with a 0.48 K temperature difference at the reference point. The conventional structure with metal heater has the lowest heating efficiency. The temperature only changed 0.36 K at reference point. Among all three test groups,

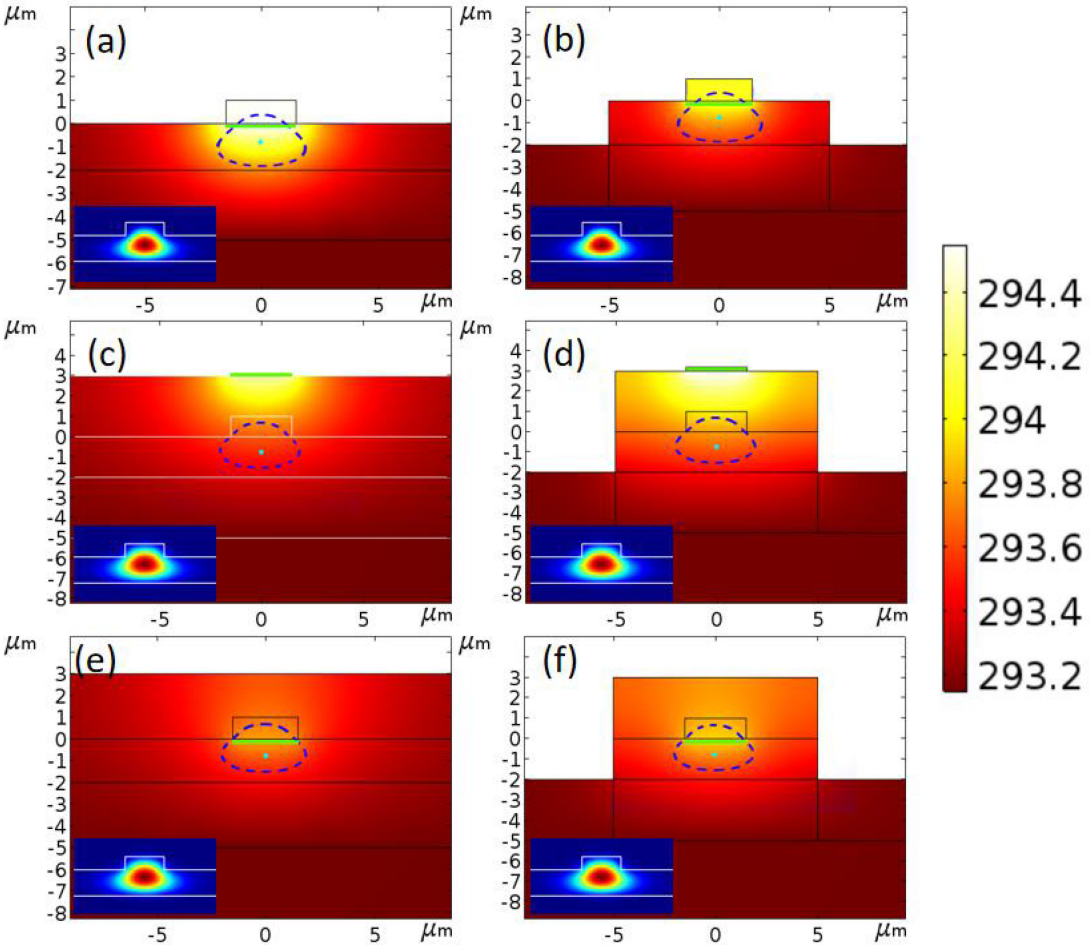

Fig. 5. Simulation results of thermal distribution with different TO structures. (a) Graphene nano-heater. (b) Graphene nano-heater with air-trench. (c) Metal heater. (d) Metal heater with air trench. (e) Graphene nano-heater with PMMA upper-cladding. (f) Graphene nano-heater with PMMA upper-cladding & air trench.

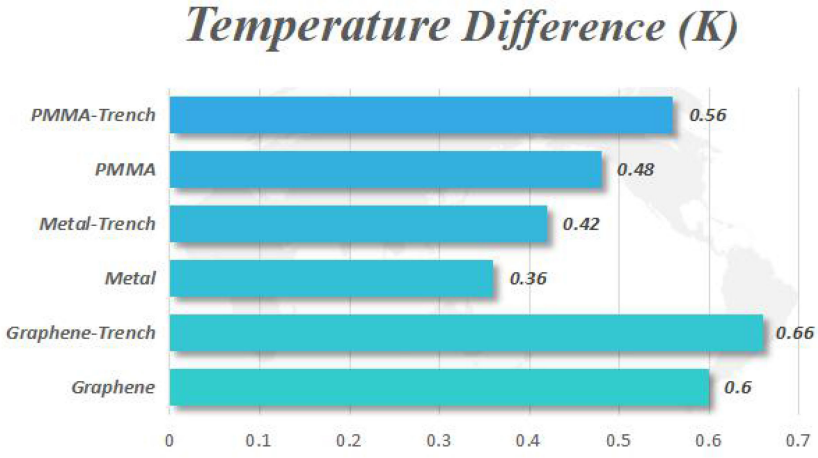

Fig. 6. Chart of temperature difference between reference point and external environment for different structures with same output power on heaters.

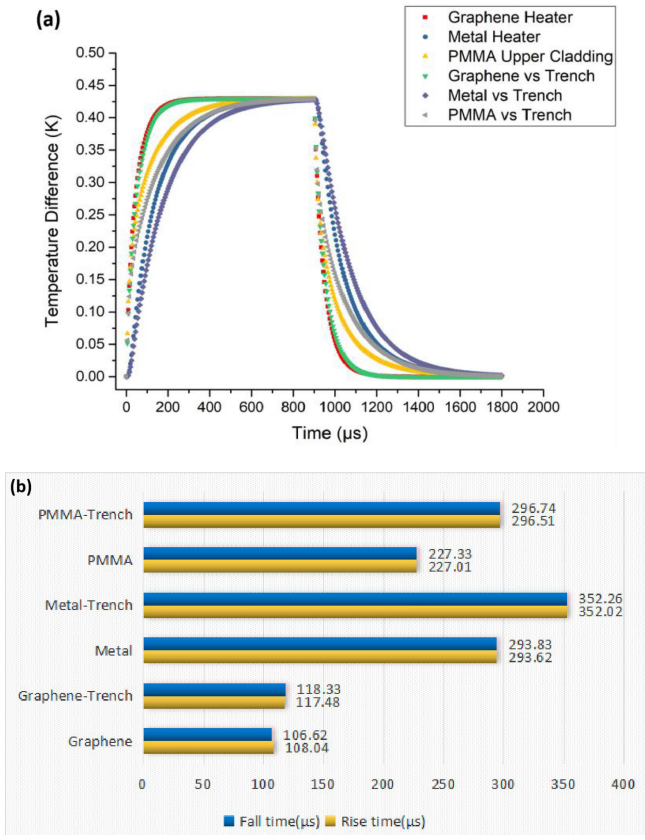

Fig. 7. (a) Transient response of temperature of MZI optical switch for different TO structure. (b) Rise time and fall time of MZI optical switch for different TO structures.

the structures with air trenches always show higher heating efficiency than the ones without air trenches.

Transient response comparison of TO optical switches for each test structure have been done as well. Waveguide temperature $T_{waveguide}$ is calculated as the average temperature of the dark blue dash line enclosed area in Fig. 5. Refractive index variation is calculated based on the equation:

$$\Delta n(x, y) = n_T(x, y) \times \Delta T(x, y) \tag{1}$$

As mentioned above, the length of MZI arms is 10 mm. ΔT that required for π phase shift is derived as 0.43 K. This is the required on/off temperature difference for the MZI optical switch. So the power on heaters are set to generate 0.43 K statistic temperature difference on waveguide area for each structure. The transient responses of such setup are shown in Fig. 7.

According to the simulation result, the proposed structure has the fastest transient response, the rise time and fall time of which are 108.04 μs and 106.62 μs, respectively. The conventional structure with metal heater has the lowest response speed. The rise time and fall time are 293.62 μs and 293.83 μs, respectively. The structure with graphene nano-heater and PMMA upper-cladding layer also show much slower transient response than the proposed structure, which means that thermal attributes of upper cladding layer could be critical to the devices' transient performance. In addition, structures with air trenches in all three comparison groups show worse performance than the ones without air trenches.

Power consumption for an effective on/off operation of the test structures is shown in Fig. 8. As can be seen, the proposed structure consumes almost half of power to complete full on/off operation comparing with the conventional structures.

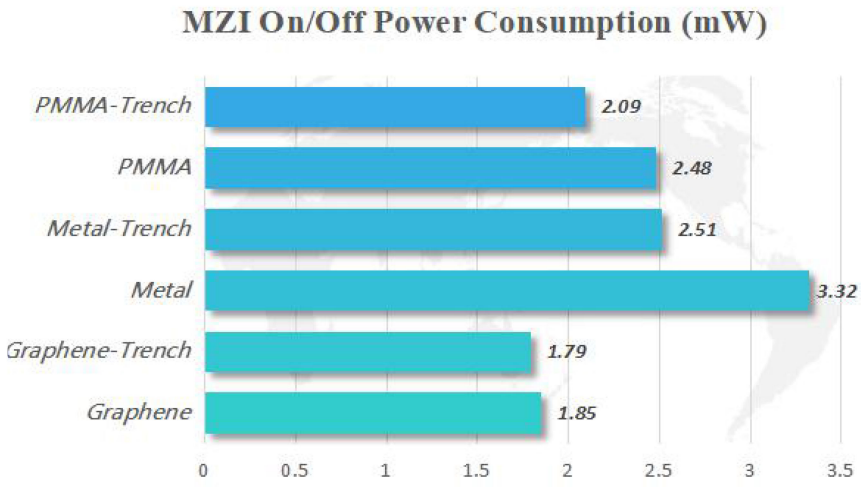

Fig. 8. Chart of on/off power consumption for MZI optical switch for different structures.

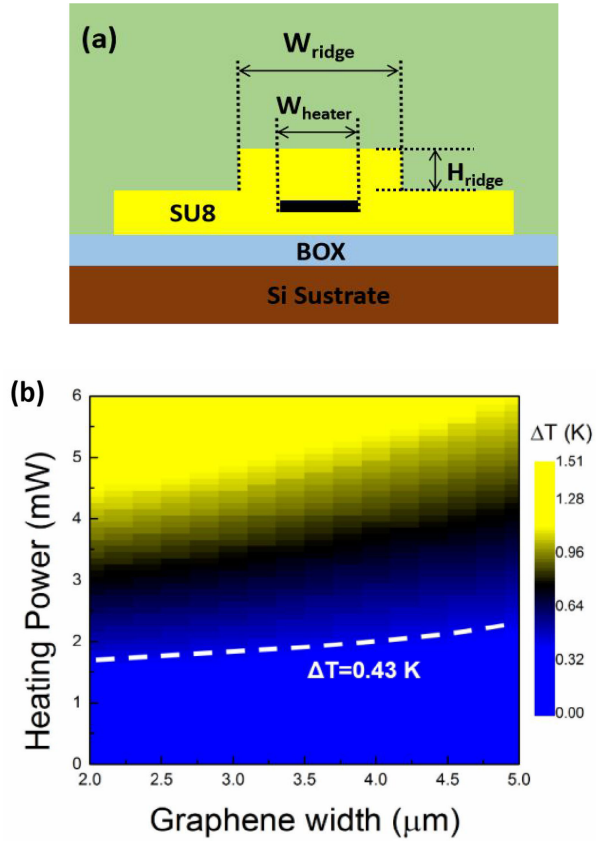

Fig. 9. (a) Proposed structure and parameter setting. (b) Temperature dependency of width of the heater and heating power.

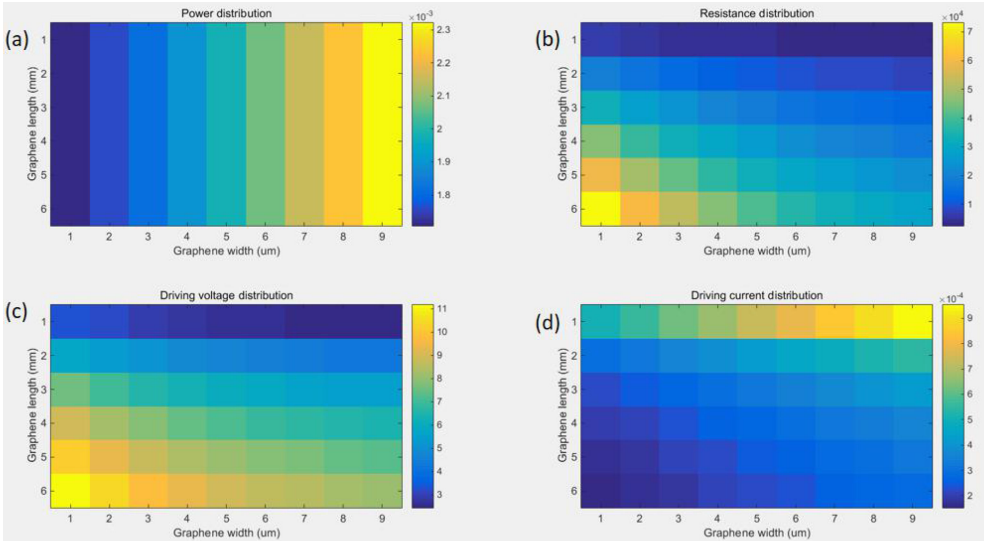

Fig. 10. (a) Heating power distribution. (b) Electrode resistance distribution. (c) Driving voltage distribution. (d) Driving current distribution with different length and width of graphene nano-heater.

To further study the proposed structure, relationship among heating power, heater's width and temperature difference has been investigated. Fig. 9(a) illustrates the condition under which the parameters is swept and analyzed. The width W_{ridge} and height H_{ridge} of ridge waveguide are set to 3 μm and 2 μm, respectively. The temperature difference's dependency on W_{heater} and heating power is shown in Fig. 9(b).

According to the results, nano-heater with wider width consumes more heating power to achieve same temperature difference, which means narrowing the nano-heaters results in higher heating efficiency.

For a novel structure, it is also critical to check the design tolerance in terms of compatible with various commercially available CMOS power supplies. As a result, the properties of the graphene nano-heater have to be calculated and approximated first.

It is worth mentioning that various publications have reported that the optical absorption coefficient of intrinsic single-layer graphene is 2.3% [35] and integration graphene with waveguide can further push this number to 0.2 dB μm^{-1} [36]. Such high optical absorption coefficient of graphene is detrimental to graphene integrated PLCs, since it may result in high on-chip optical loss. Fortunately, optical absorption of graphene can be eliminated by Pauli blocking [37], [38]. Thanks to the relatively low density of states of graphene, the Fermi level can be shifted intensely by intentional doping. When the doping of graphene is high enough to shift the Fermi level of graphene exceeding half of photon energy, graphene becomes totally transparent. In our case, doping of graphene is achieved by sandwiching graphene between polymer layers. When polymer molecules are in contact with the surface of graphene, these molecules inject carriers into graphene in order to reach thermal equilibrium, resulting in the doping of graphene [39], [40].

For graphene materials in such case, the relation between Fermi energy level and carrier density follows the equation [40]

$$E_F = \hbar \times |V_F| \times \sqrt{\pi n} \tag{2}$$

where E_F is the Fermi energy level, $v_F = 1 \times 10^6$ m·s^{-1} is the Fermi velocity and $\hbar$ is Planck constant.

For the incident light at wavelength of 1550 nm, the photon energy is approximately 0.8 eV.

According to Pauli blocking, E_F equals to 0.4 eV. Substitute E_F into equation (2), we derived $n = 4.7 \times 10^{13}$ cm^{-2}. It is worth mentioning that this is the minimum doping level to render graphene

transparent. The electric resistance of graphene nano-heater R is calculated based on the equation

$$R = \frac{L}{W} \times \frac{1}{n \cdot e \cdot \mu} \tag{3}$$

where L is the length of the nano-heater that we used in our test structure, W is the width of nano-heater, which is optimized earlier, $n = 4.7 \times 10^{13}$ cm^{-2} is the doping density of graphene, e is the elementary charge and μ is the carrier mobility of graphene. In this simulation, we assume $\mu = 1 \times 10^4$ $cm^2 \cdot V^{-1} \cdot s^{-1}$. The resistance R for different L and W can be calculated thereafter. Input electric current or voltage for different L and W, that MZI switch requires to complete an on/off operation, is then calculated based on the simulation results. Fig. 10 shows the relationship among L, W, input current I and input voltage V.

As shown in Fig. 10, the range of L and W is set to 1 mm$\sim$6 mm and 1 μm$\sim$9 μm, respectively. The maximum driving current I_{max} is 0.95 mA. The maximum driving voltage V_{max} is 11.17 V. The maximum heating power is 2.32 mW. All the maximum input parameters are within the range of commercial CMOS power supply standard, which means that the proposed structures have rather good compatibility in a very wide range.

4. Conclusion

A novel polymer/silica based thermal-optical phase modulation structure has been proposed in this paper. In addition, related fabrication process has been introduced. Furthermore, simulations of MZI optical switches with the proposed structure and the conventional structures are conducted. Results show that the proposed structure is three times faster than the conventional structures in terms of response speed, while consumes only half of power. Design tolerance and compatibility with standard CMOS power supplies has also been investigated. It shows that proposed structure and the related devices have substantial design tolerance in terms of nano-heaters' size and rather good compatibility with commercially available CMOS power supply standard.

Acknowledgment

No conflicts of interest to declare.

References

[1] Q. Huang, Y. Yeo, and L. Zhou, "Combining circuit and packet switching using a large port-count optical cross-connect for data center networks," *Opt. Commun.*, vol. 285, pp. 4268–4274, 2012.
[2] Y. Wang and X. Cao, "A study on the dynamic waveband switching in WDM network," *J. Opt. Commun. Netw.*, vol. 3, pp. 390–398, 2011.
[3] E. Pincemin *et al.*, "Multi-band OFDM transmission at 100 Gbps with sub-band optical switching," *J. Lightw. Technol.*, vol. 32, no. 12, pp. 2202–2219, Jun. 2014.
[4] Y. Lo, H. Chow, and C. Chiang, "Reconfigurable OADM and OXC designed by a new optical switch," *Opt. Fiber Technol.*, vol. 10, pp. 187–200, 2004.
[5] B.-M. Jung and J. Yao, "A two-dimensional optical true time-delay beamformer consisting of a fiber Bragg grating prism and switch-based fiber-optic delay lines," *IEEE Photon. Technol. Lett.*, vol. 21, no. 10, pp. 627–629, May 2009.
[6] Y. Sun *et al.*, "Polymer thermal optical switch for a flexible photonic circuit," *Appl. Opt.*, vol. 57, pp. 14–17, 2018.
[7] C.-M. Tsai, H. Taga, C.-H. Yang, Y.-Y. Lo, and T.-C. Liang, "Demonstration of a ROADM using cyclic. AWGs," *J. Lightw. Technol.*, vol. 29, no. 18, pp. 2780–2784, Sep. 2011.
[8] Y.-F. Liu *et al.*, "Improved performance of thermal-optic switch using polymer/silica hybrid and air trench waveguide structures," *Opt. Lett.* vol. 40, pp. 1888–1891, 2015.
[9] J. Gosciniak and S. I. Bozhevolnyi, "Performance of thermo-optic components based on dielectric-loaded surface plasmon polariton waveguides," *Sci. Rep.*, vol. 3, 2013, Art. no. 1083.
[10] Y.-F. Liu, X.-B. Wang, J. Sun, H.-J. Gu, and X.-Q. Sun, "Thermal field analysis of polymer/silica hybrid waveguide thermo-optic switch," *Opt. Commun.*, vol. 356, pp. 79–83, 2015.
[11] K. Ariki, S. Fukushima, T. Hachino, Y. Igarashi, H. Higuchi, and H. Kikuchi, "Variable optical attenuator employing a dye-doped (polymer/liquid crystal) composite film," in *Proc. IEEE Int. Broadband Photon. Conf.*, 2015, Paper no. 15418398.
[12] P.A. Morton, J. Cardenas, J.B. Khurgin, and M. Lipson, "Fast thermal switching of wideband optical delay line with no long-term transient," *IEEE Photon. Technol. Lett.*, vol. 24, no. 6, pp. 512–514, Mar. 2012.

[13] S.-K. Liaw, Y.-T. Lai, C.-L. Chang, and O. Shung, "AWG-based WDM-PON monitoring system using an optical switch and a WDM filter," *Laser Phys.*, vol. 18, pp. 1052–1055, 2008.
[14] F. Bonaccorso, Z. Sun, T. Hasan, and A. C. Ferrari, "Graphene photonics and optoelectronics," *Nat. Photon.*, vol. 4, pp. 611–622, 2010.
[15] Q. L. Bao and K. P. Loh, "Graphene photonics, plasmonics, and broadband optoelectronic devices," *ACS Nano*, vol. 6, pp. 3677–3694, 2012.
[16] A. K. Geim and K. S. Novoselov, "The rise of graphene," *Nat. Mater.*, vol. 6, pp. 183–191, 2007.
[17] K. S. Novoselov *et al.*, "Electric field effect in atomically thin carbon films," *Science*, vol. 306, pp. 666–669, 2004.
[18] K. I. Bolotin *et al.*, "Ultrahigh electron mobility in suspended graphene," *Solid State Commun.*, vol. 146, pp. 351–355, 2008.
[19] X. Du, I. Skachko, A. Barker, and E. Y. Andrei, "Approaching ballistic transport in suspended graphene," *Nat. Nanotechnol.*, vol. 3, pp. 491–495, 2008.
[20] A. A. Balandin, "Thermal properties of graphene and nanostructured carbon materials," *Nat. Mater.*, vol. 10, pp. 569–581, 2011.
[21] D. L. Nika, E. P. Pokatilov, A. S. Askerov, and A. A. Balandin, "Phonon thermal conduction in graphene: Role of Umklapp and edge roughness scattering," *Phys. Rev. B*, vol. 79, 2009, Art. no. 155413.
[22] A. A. Balandin *et al.*, "Superior thermal conductivity of single-layer graphene," *Nano Lett.*, vol. 8, pp. 902–907, 2008.
[23] M. M. Sadeghi, M. T. Pettes, and L. Shi, "Thermal transport in graphene," *Solid State Commun.*, vol. 152, pp. 1321–1330, 2012.
[24] S. Ghosh *et al.*, "Extremely high thermal conductivity of graphene: Prospects for thermal management applications in nanoelectronic circuits," *Appl. Phys. Lett.*, vol. 92, 2008, Art. no. 151911.
[25] J. Kang *et al.*, "Heat removal in silicon-on-insulator integrated circuits with graphene lateral heat spreaders," *IEEE Electron. Device Lett.*, vol. 30, no. 12, pp. 1281–1283, Dec. 2009.
[26] R. Prasher, "Graphene spreads the heat," *Science*, vol. 328, pp. 185–186, 2010.
[27] Choi, and B. H. Hong, "High-performance graphene-based transparent flexible heaters," *Nano Lett.*, vol. 11, pp. 5154–5158, 2011.
[28] D. Sui, Y. Huang, L. Huang, J. J. Liang, Y. F. Ma, and Y. S. Chen, "Flexible and transparent electrothermal film heaters based on graphene materials," *Small*, vol. 7, pp. 3186–3192, 2011.
[29] L. Yu, J. Zheng, Y. Xu, D. Dai S. He, "Local and nonlocal optically induced transparency effects in graphene–silicon hybrid nanophotonic integrated circuits," *ACS Nano*, vol. 8, no. 11, pp. 11386–11393, 2014.
[30] Y. Sun *et al.*, "A low-power consumption MZI thermal optical switch with a graphene-assisted heating layer and air trench," *RSC Adv.*, vol. 7, pp. 39922–39927, 2017.
[31] Y. Longhai and Y. Yin, Y. Shi, D. Dai, and S. He, "Thermally tunable silicon photonic microdisk resonator with transparent graphene nanoheaters," *Optica*, vol. 2, no. 3, pp. 159–166, 2016.
[32] S. Gan *et al.*, "A highly efficient thermo-optic microring modulator assisted by graphene," *Nanoscale.*, vol. 7, pp. 20249–20255, 2015.
[33] Q. Fang, J. F. Song, and T.-Y. Liow, "Ultralow power silicon photonics thermo-optic switch with suspended phase arms," *IEEE Photon. Technol. Lett.*, vol. 23, no. 8, pp. 525–527, 2011.
[34] R. R. Nair, P. Blake, A. N. Grigorenko, and K. S. Novoselov, "Fine structure constant defines visual transparency of graphene," *Sci. Express*, vol. 10, p. 1308, 2008.
[35] H. Li, Y. Anugrah, and J. K. Steven, "Optical absorption in graphene integrated on silicon waveguides," *Appl. Phys. Lett.*, vol. 101, 2012, Art. no. 111110.
[36] W. Li, B. Chen, and C. Meng, "Ultrafast all-optical graphene modulator," *Nano Lett.*, vol. 14, pp. 955–959, 2014.
[37] R. Kou, Y. Hori, T. Tsuchizawa, K. Warabi, Y. Kobayashi, and Y. Harada, "Ultra-fine metal gate operated graphene optical intensity modulator," *Appl. Phys. Lett.*, vol. 109, 2016, Art. no. 251101.
[38] J. Moser, A. Barreiro, and A. Bachtold, "Current-induced cleaning of graphene," *Appl. Phys. Lett.*, vol. 91, 2007, Art. no. 163513.
[39] Y.-C. Lin, C.-C. Lu, and C.-H. Yeh, "Graphene annealing: how clean can it be?" *Nano Lett.*, vol. 12, pp. 414–419, 2012.
[40] P. Wei, W. Bao, Y. Pu, C. N. Lau, and J. Shi, "Anomalous thermoelectric transport of Dirac particles in graphene," *Phys. Rev. Lett.*, vol. 102, no. 16, 2009, Art. no. 166808.